PIBB 生物化学与生物物理进展
Progress in Biochemistry and Biophysics
2017, 44(6): 534~536
www.pibb.ac.cn

Study on The Relationship of Laser Power Density and Localization Precision in PALM Imaging

Dear Editor,

Photoactivated localization microscopy (PALM) improves the resolution of microscope to 2 –25 nm with the facility of photoactivated fluorescent proteins (PAFPs) [1]. PALM, stochastic optical reconstruction microscopy(STORM)[2] and fluorescence photoactivation localization microscopy (FPALM) [3] are all based on single molecule localization technique. The localization precision of single molecule localization microscopy (SMLM) depends on the photon output of fluorescent probes and background noise, as illuminated in the following formula[4]:

$$\left(\sigma_{x,y}^2\right)_m \approx \frac{s^2+a^2/12}{N_m}+\frac{4\sqrt{\pi}\,s^3 b_m^2}{aN_m^2} \qquad (1)$$

Where $\sigma_{x,y}$ is the standard deviation of localization; N_m is the total photon number; b_m is the background noise level; a is the pixel size in the image (taking into account the system magnification); s is the standard deviation of PSF. As the optical properties of PAFPs and background noise are related to excitation laser power density, we design a series of experiments to study the relationship between laser power density and localization precision in PALM imaging.

Generally, PAFPs are divided into three types, photoactivatable, photoconvertable and photoswitchable[5-6]. There are many new PAFPs of each type being developed to improve the resolution, including Dronpa, PAmCherry and mEos3.2[7–9]. We selected and purified most widely used PAFPs(Table S1) for further single molecule imaging test.

PAFPs were purified as previously described [9]. Single molecule imaging of PAFPs was performed with TIRFM at room temperature. Cover slips were cleaned seriously and placed in the sample holder of PALM instrument. Additional PBS(pH 7.4) was added to the sample chamber after spreading the samples on the cover slip. We chose 561 nm excitation laser power density from 0.1 to 2.0 kw/cm^2 for red PAFPs and 488 nm excitation laser power density from 0.01 to 2.5 kw/cm^2 for green PAFPs. After image acquisition, all molecules were identified and fitted with a 2D Gaussian fitting [10] to obtain the position, number of photons (N_m) and s of the point spread function. The background noise level (b_m) was determined by calculating the s of the intensity of an illuminated area where no single molecule is visible. Finally, the 2D localization precision for each molecule could be obtained with equation (1).

To get high localization precision, it is important to maximize the photon yield of the fluorophores. We found that total photon number of selected PAFPs increased when increasing the excitation laser power, but saturated after the laser power passed a threshold (Figure 1a –c). PAmCherry and PATagRFP show decreased photon output with higher laser power density (Figure 1c), which is different from other PAFPs. This may due to low laser tolerance of red irreversible photoactivatable PAFPs. Excitation light may have bleaching effect on fluorescent molecules, suitable excitation laser power density should be chosen to maximize the photon output of specific fluorophores to get best localization precision.

Background noise level is affected by autofluorescence of the sample and residual fluorescence of surrounding probe molecules in the

dark state. For fluorophores with low contrast ratios, the collective fluorescence from dark molecules can obscure the signal from the small number of bright molecules during each imaging cycle [11]. We found these kind of background noise is positively related to laser power density (Figure 1d～f).

As in formula (1), our results showed that in order to get high localization precision, appropriate excitation power needs to be chosen to balance the number of photons detected from activated PAFPs and the background noise. We found the optimal localization precision can be achieved at around 0.5 kw/cm^2 laser power density for selected red PAFPs (Figure 1g～i, Table 1). For green PAFPs, mGeos-M delivers the highest localization precision at very low laser power. It shows that mGeos-M is suitable for live cell imaging which is sensitive to photo toxicity (Figure 1h, Table 1). We further verified our results with large quantity single molecule imaging data at their optimal laser power density respectively (Figure S1–S6).

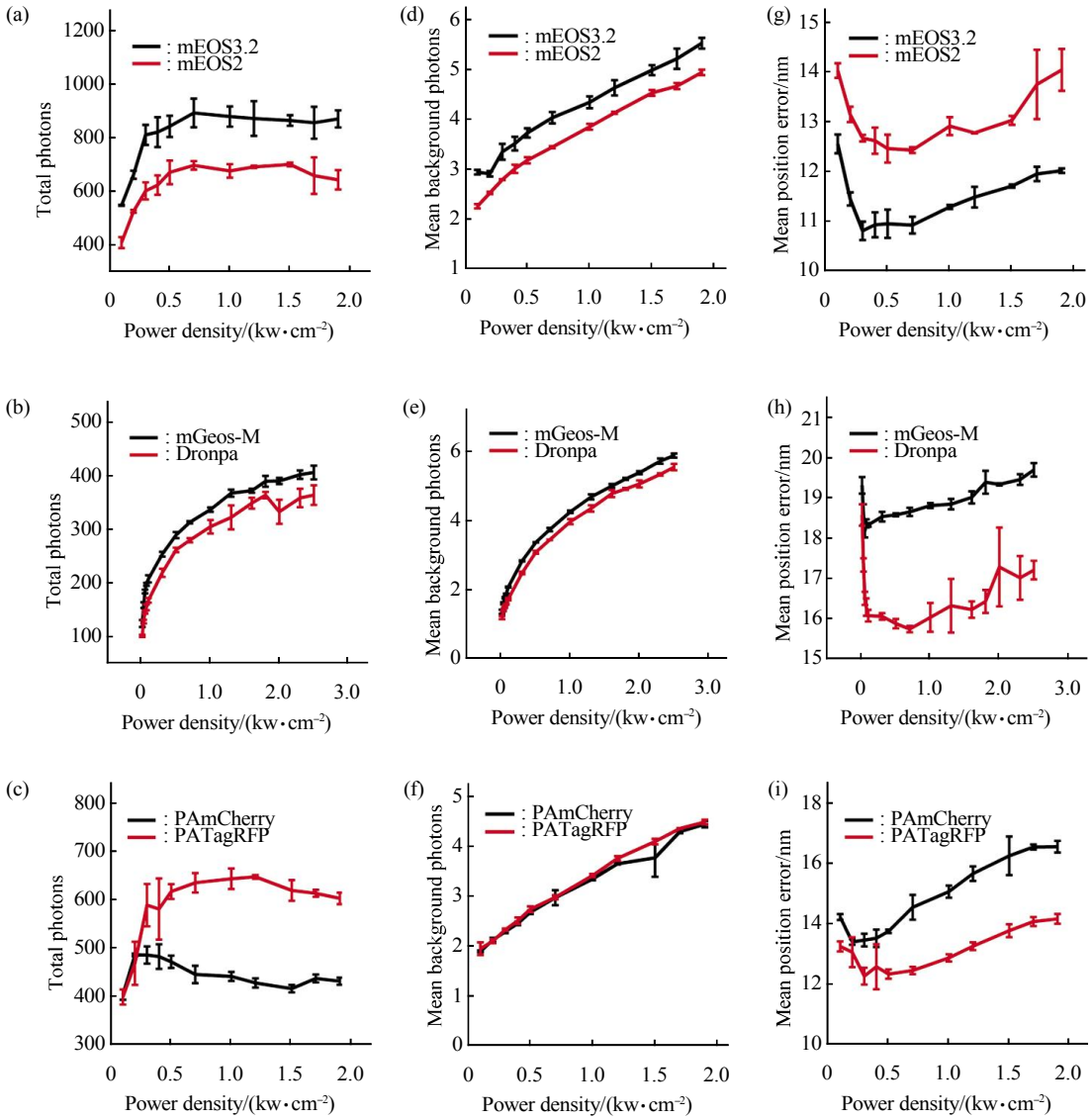

Fig. 1 Effects of the excitation laser power density on the number of photons detected from PAFPs, background noise and localization precision

Total photons(a–c), background photons(d–f) and position error(g–i) of photoconvertable FPs(a, d, g), photoswitchable FPs(b, e, h), photoactivatable FPs (c, f, i).

Table 1 Optical localization precision of PAFPs at different laser power density

PAFPs	Photoconvertable FPs		Photoswitchable FPs		Photoactivatable FPs	
	mEos2	mEos3.2	mGeos-M	Dronpa	PAmCherry	PATagRFP
Laser power density/(kw·cm^{-2})	0.7	0.7	0.05	0.7	0.2	0.3
Position error/nm	12.42	10.92	18.19	15.75	13.44	12.30

In summary, we selected several mostly used PAFPs and studied the relationship between laser power density and their localization precision in PALM imaging. These results can guide researchers to choose appropriate laser power densities for specific PAFPs in PALM imaging and achieve optimal resolution.

Acknowledgements This work was financially supported by grants from the National Key Research and Development Program of China (2016YFA0502400) , Natural Science Foundation of China (81427802 31270884, 30900268 and 31400658), the Beijing Natural Science Foundation (5122026, 5092017), and the Youth Innovation Promotion Association of the Chinese Academy of Sciences (2011087).

Supplementary material Table S1, Figures S1–S6 are araillable at paper online(http://www.pibb.ac.cn).

DOI: 10.16476/j.pibb.2017.0153

FAN Chun-Yan[1, 2)*], LI Yuan-Yuan[1)*], GU Lu-Sheng[3)*], LI Wei-Xing[3)], XU Xiao-Jun[1)], ZHANG Shu-Wen[1, 2)], WANG Lei[4)],CHEN Yan[5)], XUE Yan-Hong[1, 2)**], JI Wei[2, 3)**]

[1)] National Laboratory of Biomacromolecules, Institute of Biophysics, Chinese Academy of Sciences, Beijing 100101, China;

[2)] University of Chinese Academy of Sciences, Beijing 100049, China;

[3)] Center for Biological Instrument Development, Institute of Biophysics, Chinese Academy of Sciences, Beijing 100101,China;

[4)] Foshan University, Foshan 528000, China;

[5)] Jiangsu Academy of Science and Technology for Development, Nanjing 210042, China

*These authors contributed equally to this work.

**Correspondence to:

JI Wei. Tel: 86-10-64888846, E-mail: jiwei@ibp.ac.cn

XUE Yan-Hong. Tel: 86-10-64888846

E-mail: xueyanhong@ibp.ac.cn

Received: April 23, 2017 Accepted: May 16, 2017

References

[1] Betzig E, Patterson G H, Sougrat R, *et al*. Imaging intracellular fluorescent proteins at nanometer resolution. Science, 2006, **313**(5793): 1642−1645

[2] Rust M J, Bates M, Zhuang X. Sub-diffraction-limit imaging by stochastic optical reconstruction microscopy (STORM). Nature Methods, 2006, **3**(10): 793−795

[3] Hess S T, Girirajan T P, Mason M D. Ultra-high resolution imaging by fluorescence photoactivation localization microscopy. Biophysical Journal, 2006, **91**(11): 4258−4272

[4] Thompson R E, Larson D R, Webb W W. Precise nanometer localization analysis for individual fluorescent probes. Biophysical Journal, 2002, **82**(5): 2775−2783

[5] Hedde P N, Nienhaus G U. Super-resolution localization microscopy with photoactivatable fluorescent marker proteins. Protoplasma, 2014, **251**(2): 349−362

[6] Nienhaus K, Nienhaus G U. Fluorescent proteins for live-cell imaging with super-resolution. Chemical Society Reviews, 2014, **43**(4): 1088−1106

[7] Habuchi S, Ando R, Dedecker P, *et al*. Reversible single-molecule photoswitching in the GFP-like fluorescent protein Dronpa. Proc Natl Acad Sci USA, 2005, **102**(27): 9511−9516

[8] Subach F V, Patterson G H, Manley S, *et al*. Photoactivatable mCherry for high-resolution two-color fluorescence microscopy. Nature Methods, 2009, **6**(2): 153−159

[9] Zhang M, Chang H, Zhang Y, *et al*. Rational design of true monomeric and bright photoactivatable fluorescent proteins. Nature Methods, 2012, **9**(7): 727−729

[10] Smith C S, Joseph N, Rieger B, *et al*. Fast, single-molecule localization that achieves theoretically minimum uncertainty. Nature Methods, 2010, **7**(5): 373−375

[11] Fernandez-Suarez M, Ting A Y. Fluorescent probes for super-resolution imaging in living cells. Nat Rev Mol Cell Biol, 2008, **9**(12): 929−943

Supplements

Table S1 Properties of selected proteins

PAFPs	Pre-/post activation color	Activation light	Absorbance/emission peaks(nm)	Oligomeric status	Reference
Photoconvertable fluorescent proteins					
mEos2			506/519 (G) 573/584 (R)	Monomer	[1]
mEos3.2			518/525 (G) 585/591 (R)	Monomer	[2]
Photoswitchable fluorescent proteins					
Dronpa			503/522	Monomer	[3]
mGeos-M			503/514	Monomer	[4]
Photoactivatable fluorescent proteins					
PAmCherry			564/595	Monomer	[5]
PATagRFP			562/595	Monomer	[6]

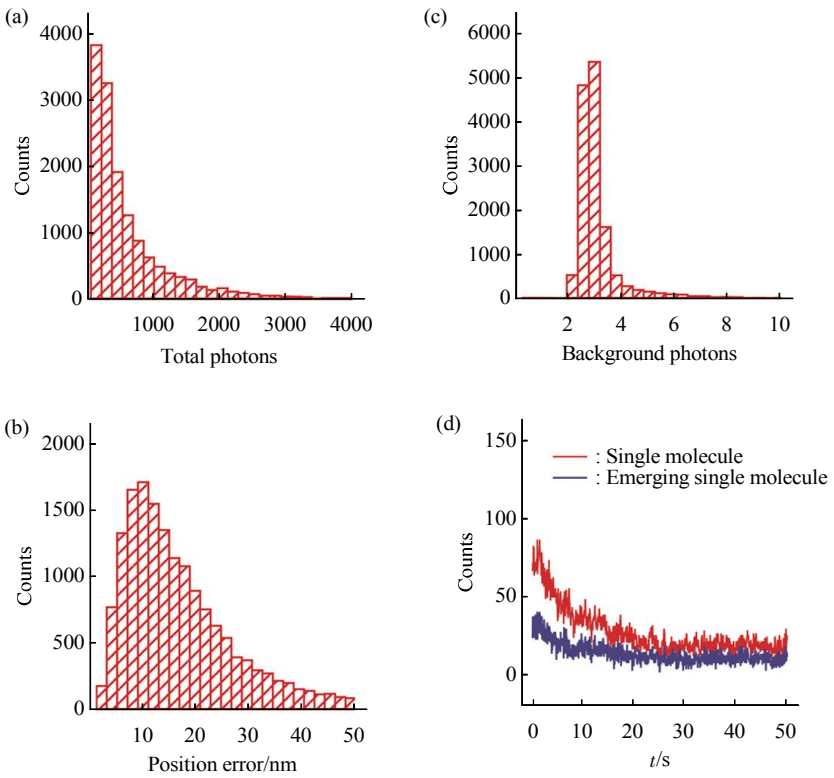

Figure S1 Single molecule properties of mEos2 at optimal laser power density

Distribution of total photons (a), background photons (b), position error (c), number of single molecules per frame (0.05 s) and emerging molecules per frame (0.05 s) (d).

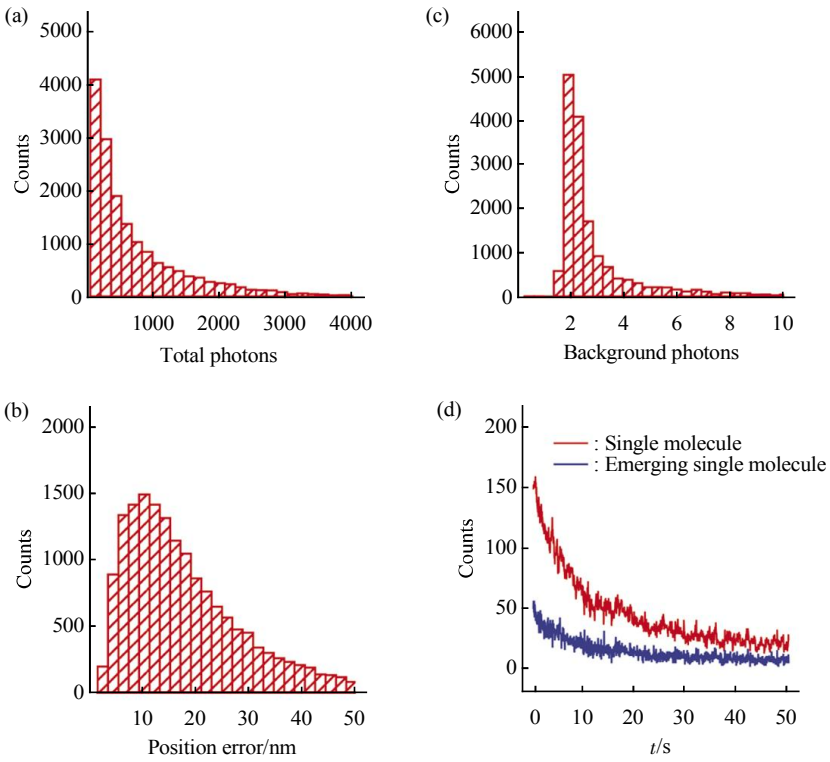

Figure S2 Single molecule properties of mEos3.2 at optimal laser power density

Distribution of total photons (a), background photons (b), position error (c), number of single molecules per frame (0.05 s) and emerging molecules per frame (0.05 s) (d).

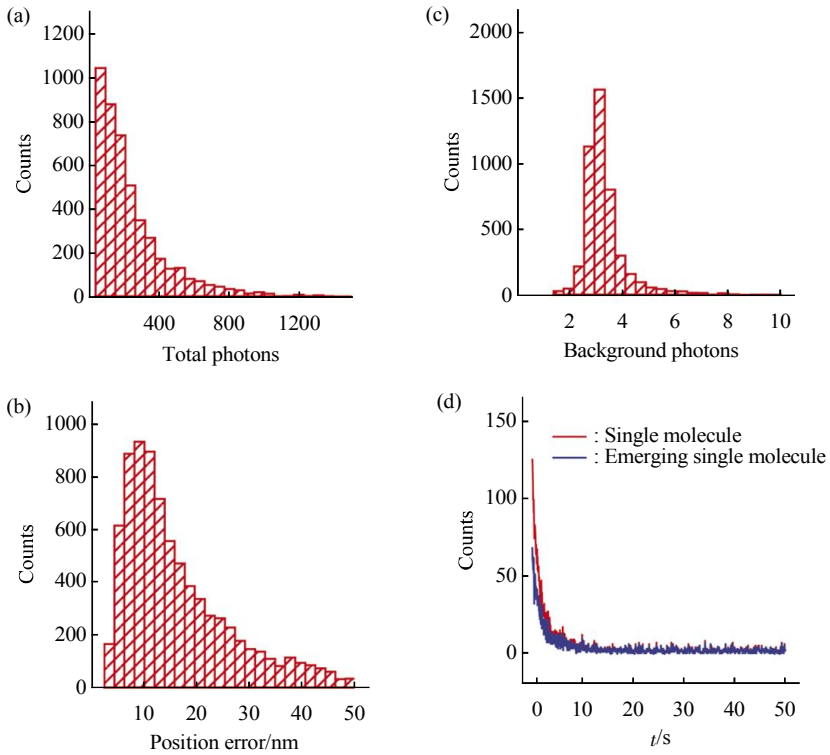

Figure S3 Single molecule properties of Dronpa at optimal laser power density

Distribution of total photons (a), background photons (b), position error (c), number of single molecules per frame (0.05 s) and emerging molecules per frame (0.05 s) (d).

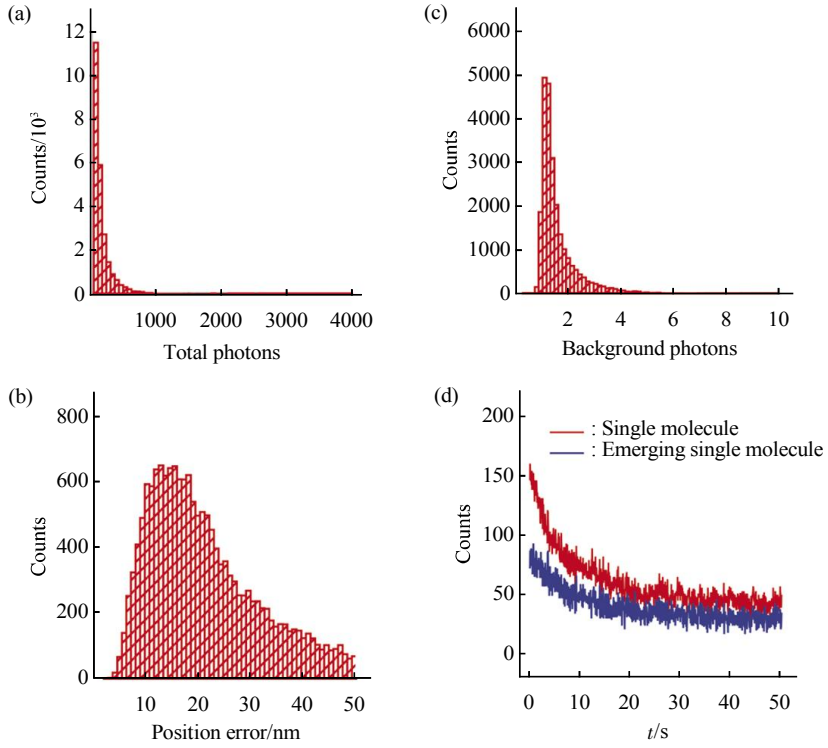

Figure S4 Single molecule properties of mGeosM at optimal laser power density

Distribution of total photons (a), background photons (b), position error (c), number of single molecules per frame (0.05 s) and emerging molecules per frame (0.05 s) (d).

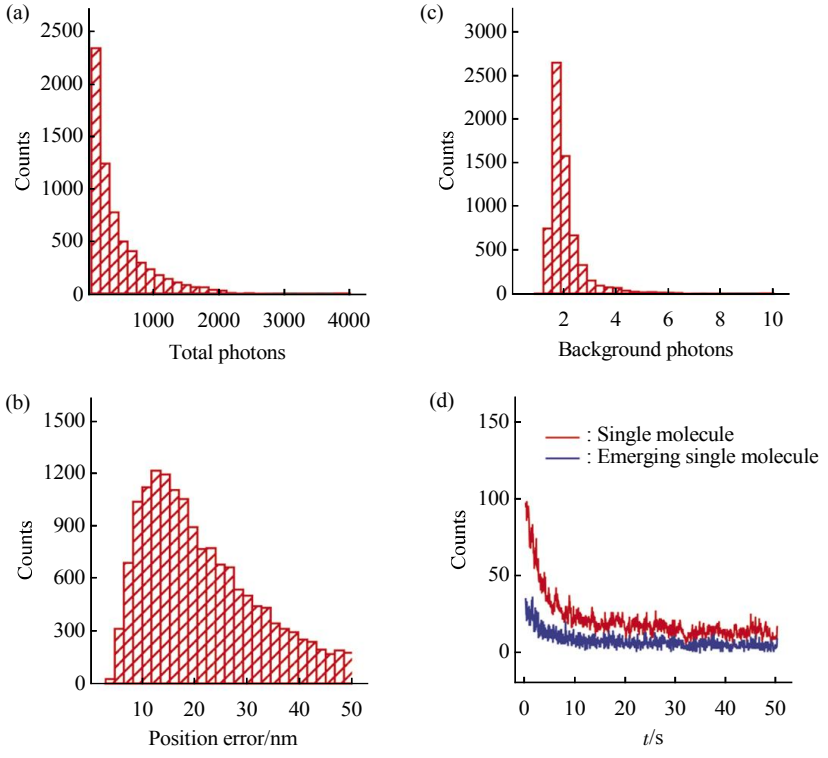

Figure S5 Single molecule properties of PAmCherry at optimal laser power density

Distribution of total photons (a), background photons (b), position error (c), number of single molecules per frame (0.05 s) and emerging molecules per frame (0.05 s) (d).

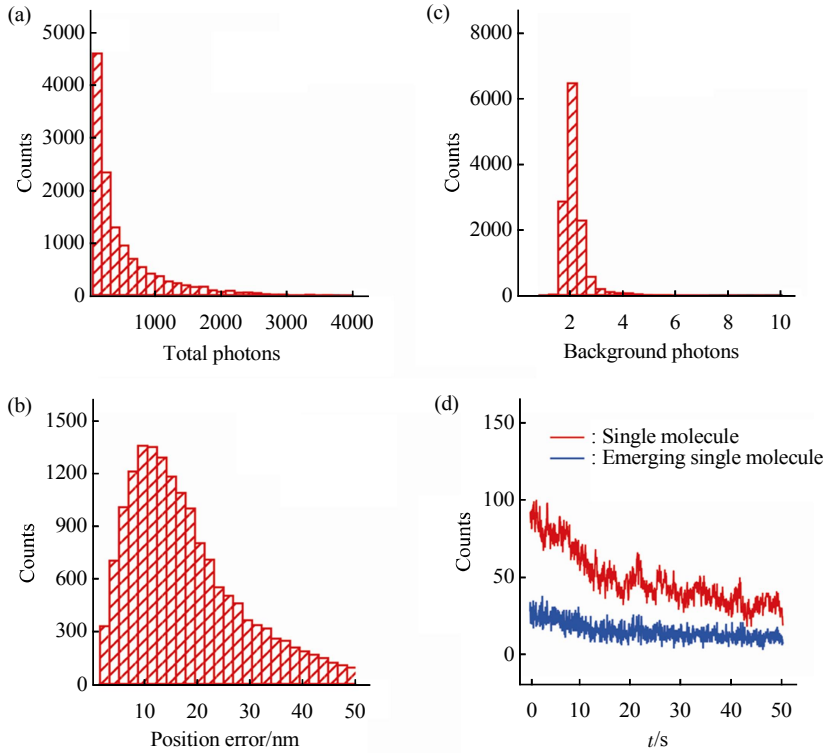

Figure S6 Single molecule properties of PATagRFP at optimal laser power density

Distribution of total photons (a), background photons (b), position error (c), number of single molecules per frame (0.05 s) and emerging molecules per frame (0.05 s) (d).

References

[1] Mckinney S A, Murphy C S, Hazelwood K L, *et al*. A bright and photostable photoconvertible fluorescent protein. Nature Methods, 2009, **6**(2): 131−133

[2] Zhang M, Chang H, Zhang Y, *et al*. Rational design of true monomeric and bright photoactivatable fluorescent proteins. Nature Methods, 2012, **9**(7): 727−729

[3] Habuchi S, Ando R, Dedecker P, *et al*. Reversible single-molecule photoswitching in the GFP-like fluorescent protein Dronpa. Proc Natl Acad Sci USA, 2005, **102**(27): 9511−9516

[4] Chang H, Zhang M, Ji W, *et al*. A unique series of reversibly switchable fluorescent proteins with beneficial properties for various applications. Proc Natl Acad Sci USA, 2012, **109** (12): 4455−4460

[5] Subach F V, Patterson G H, Manley S, *et al*. Photoactivatable mCherry for high-resolution two-color fluorescence microscopy. Nature Methods, 2009, **6**(2): 153−159

[6] Subach F V, Patterson G H, Renz M, *et al*. Bright monomeric photoactivatable red fluorescent protein for two-color super-resolution sptPALM of live cells. Journal of the American Chemical Society, 2010, **132**(18): 6481−6491